Inhibition of histone readers bromodomain extra-terminal proteins alleviates scleroderma fibrosis

Sirapa Vichaikul[1], Pamela J. Palisoc[1], Mustafa Ali[1], Phillip L. Campbell[1], M. Asif Amin[1], Jeffrey H. Ruth[1], Dallas M. Rohraff[1], Jonatan L. Hervoso[1], David A. Fox[1], Dinesh Khanna[1,2], Amr H. Sawalha[3,4,5], and Pei-Suen Tsou[1]

[1]Division of Rheumatology, Department of Internal Medicine, University of Michigan, Ann Arbor, MI

[2]University of Michigan Scleroderma Program, Ann Arbor, MI

[3]Division of Rheumatology, Department of Pediatrics, University of Pittsburgh School of Medicine, UPMC Children's Hospital of Pittsburgh, Pittsburgh, PA, USA

[4]Division of Rheumatology and Clinical Immunology, Department of Medicine, University of Pittsburgh School of Medicine, Pittsburgh, PA, USA

[5]Lupus Center of Excellence, University of Pittsburgh School of Medicine, Pittsburgh, PA, USA

Address correspondence: Pei-Suen Tsou, Division of Rheumatology, University of Michigan, 109 Zina Pitcher Pl, 4025 BSRB, Ann Arbor, MI 48109, USA. Telephone (734) 647-1192. Email: ptsou@umich.edu.

Key Words: Scleroderma, histone readers, bromodomain extra-terminal proteins, fibrosis, fibroblasts

Classification: Biological Sciences/ Immunology and Inflammation

Abstract

Objectives: Binding of the bromodomain and extra-terminal domain proteins (BETs) to acetylated histone residues is critical for gene transcription in many fibrotic diseases. This study sought to determine the anti-fibrotic efficacy and potential mechanisms of BET inhibition in scleroderma (SSc).

Methods: Dermal fibroblasts were isolated from biopsies from healthy subjects or patients with diffuse cutaneous (dc)SSc. Fibroblasts were treated with pan BET inhibitor JQ1, BRD2 inhibitor BIC1, or BRD4 inhibitors AZD5153 or ARV825. Knockdown of BETs was achieved by siRNA transfection. The *in vivo* anti-fibrotic efficacy of JQ1 was determined in a bleomycin-induced skin fibrosis mouse model. T-test or ANOVA were used to compare differences between groups, and a p-value of <0.05 was considered significant.

Results: BET inhibitor JQ1 dose-dependently downregulated pro-fibrotic genes in dcSSc fibroblasts, and inhibited cell migration and gel contraction. It suppressed proliferation by inducing cell cycle arrest. The anti-fibrotic effects of JQ1 were also observed in TGFβ-treated normal fibroblasts. JQ1 prevented bleomycin-induced skin fibrosis in mice. The anti-fibrotic effect of JQ1 was mediated by inhibition of BRD4, as specific blockade or knockdown of BRD4 led to downregulation of fibrotic markers and inhibition of myofibroblast properties, while inhibition or knockdown of BRD2 or BRD3 had minimal effects in dcSSc fibroblasts.

Conclusions: BET inhibition showed promising anti-fibrotic effects in SSc both *in vitro* and *in vivo.* Specifically, we showed that BRD4 plays a critical role in SSc fibrosis and that targeting BRD4 might be a novel therapeutic option for this disease.

Significance statement

Blockade of histone readers bromodomain extra-terminal proteins (BETs) shows potent anti-fibrotic properties in SSc dermal fibroblasts and bleomycin-induced skin fibrosis model. Among the BETs, BRD4 appears to regulate essential processes involved in SSc fibrosis. Results from this study provide the scientific foundation for the use of BET or BRD4 inhibitors in treating SSc.

Introduction

Systemic sclerosis (scleroderma, SSc) is an autoimmune disease characterized by vascular dysfunction as well as excessive synthesis and deposition of extracellular matrix (ECM) in affected organs. Activation of the immune system and vasculopathy precede fibrosis, in which fibroblast activation and subsequent myofibroblast transdifferentiation are necessary events. At present, SSc is not curable; current treatments focus on managing disease manifestations in an effort to ease the progression of tissue remodeling.

Although the exact etiology of the disease is not known, a growing body of literature has been pointing to the critical involvement of epigenetic mechanisms in SSc pathogenesis (1). Epigenetic regulation affects chromatin dynamics and thereby modulates gene transcription. In addition to DNA methylation and non-coding RNAs, histone changes are implicated in SSc fibroblast activation (2-4). Acetylation of histones on lysine residues is one of the most common histone modifications that relaxes the chromatin structure by loosening the histone-DNA interaction, which results in increased chromatin accessibility for transcription. Dysregulation of histone acetylation could result in aberrant gene expression leading to pathogenic consequences. These histone marks are therefore tightly regulated by a set of histone acetyltransferases and histone deacetylases. They are also controlled by proteins containing the bromodomain module, such as the bromodomain extra-terminal domain (BET) family proteins. The four members of the BETs, BRD2, BRD3, BRD4, and the testis-specific BRD-t, share a common domain consisting of two N-terminal bromodomains, BD1 and BD2, that bind to acetylated lysine residues on histones. These histone readers provide scaffolds to

attract components of the transcriptional machinery to histone acetylation marks. Pharmacological inhibition of BET proteins could result in repression of downstream gene expression, thereby modulating various physiological conditions. Indeed, prototype BET inhibitors such as JQ1 or I-BET attenuated various types of cancer and tissue fibrosis (5-9).

Considering the potential anti-fibrotic properties of BET inhibition, we investigated whether BET inhibitor JQ1 can modulate fibrogenesis in diffuse cutaneous SSc (dcSSc) fibroblasts and in an animal model of SSc. We posit that BET inhibition impedes the expression of pro-fibrotic genes and blocks myofibroblast differentiation in SSc, thereby improves fibrosis (**Figure 1**). Further, we demonstrated the involvement of BRD4 in mediating the pro-fibrotic effect of BETs and identify BRD4 as a novel therapeutic target for SSc.

Results

Anti-fibrotic properties of BET inhibition in dermal fibroblasts. To evaluate the effect of BET proteins in dermal fibroblasts, we used a pan-BET inhibitor, JQ1, to treat dcSSc fibroblasts. We evaluated the expression of pro-fibrotic genes *COL1A1*, *ACTA2, CTGF,* and *TGFB1,* as well as collagen-degrading enzyme *MMP1* and its inhibitor *TIMP3.* Inhibition of BET by JQ1 led to a dose-dependent decrease in fibrotic markers including *COL1A1*, *ACTA2, and CTGF*, suggesting that JQ1 is anti-fibrotic in these cells (**Figure 1B**). In addition, JQ1 also increased *MMP1*, which is critical for collagen turnover, while it had minimal effect on *TIMP3*. Interestingly JQ1, at the highest dose, significantly increased *TGFB1*. This might be an off-target effect of the inhibitor at high doses. Given that this dose (22 µM) had minimal effect on *CTGF*, we postulate that the doses between 0.1-1 µM might be most effective in blocking fibrosis in these cells.

To further characterize the anti-fibrotic effect of JQ1 in dcSSc fibroblasts, we performed several functional assays. Treatment with JQ1 dose-dependently reduced migration of dcSSc fibroblasts (**Figure 2A**) and decreased cell proliferation (**Figure 2B**). The mechanism of reducing cell proliferation by JQ1 might be in part due to its effect on inducing apoptosis, as JQ1 dose dependently increased apoptotic cells as indicated by green fluorescence released by activated caspase-3/7 using IncuCyte® (**Figure 2C**). However, this effect appears to be delayed, as apoptotic cells appeared after 40 hours while differences in cell proliferation became evident after 30 hours of JQ1 treatment (**Figure 2B** vs. **2C**). This suggests that other mechanisms are involved in the effect of JQ1 on cell growth. To further analyze the effect of JQ1 on cell growth, we used PI to analyze cell cycle distribution in dcSSc fibroblasts. JQ1 induced a reduction in cells in

the S-phase and accumulation of cells in the G1/G0 phase (**Figure 2D**). In addition to cell migration and proliferation, we also examined the effect of JQ1 on gel contraction. Treatment of dcSSc fibroblasts with JQ1 resulted in decrease in gel contraction (**Figure 2E**), with 0.5 μM being the most effective concentration.

Since TGFβ is critical in promoting fibrosis in SSc, we treated normal dermal fibroblasts with TGFβ to induce a myofibroblast phenotype. This was confirmed with an increase in cell migration, proliferation, as well as gel contraction in these TGFβ-treated normal fibroblasts compared to non-treated controls (**Figure 2F-H**). Co-treatment with JQ1 significantly reduced TGFβ-induced migration, proliferation, and gel contraction in normal dermal fibroblasts. Of note we chose to use 1 μM of JQ1 in this set of experiments since this dose appears to be most consistent in inhibiting fibrosis without inducing *TGFB1* in dcSSc fibroblasts.

The anti-fibrotic effects of JQ1 in bleomycin-treated mice. To further investigate the anti-fibrotic effect of BET inhibition, we tested JQ1 in an animal model of fibrosis. Daily injection of bleomycin in a defined area in the back of mice increased dermal thickness and collagen accumulation (**Figure 2I**). Daily JQ1 oral gavage resulted in prevention of skin fibrosis in bleomycin-treated mice, as significantly reduced dermal thickness and collagen deposition were observed. In addition, immunofluorescent staining of the skin sections revealed increased αSMA- and F4/80-positive cells in bleomycin-treated mice, with F4/80 staining reaching statistical significance (**Figure 2J**). These results were also reflected at the mRNA level, as pro-fibrotic genes including *Acta2* and *Col1a1* that were significantly elevated in bleomycin-treated mice, were downregulated in the presence of

JQ1 (**Table 2**). However, there was no difference in *Ctgf* expression between the groups.

BET expression in SSc. We examined the expression of BET proteins in dermal fibroblasts. Out of the four BETs, BRD-t is expressed predominantly in the testis therefore excluded from our study. At the mRNA level, only *BRD4* was significantly upregulated in dcSSc fibroblasts compared to normal fibroblasts (**Figure 3A**). At the protein level, however, the expression of the BETs was variable in dcSSc fibroblasts and none of them were different from cells from healthy subjects (**Figure 3B**).

BRD4 is anti-fibrotic. Since JQ1 is a pan-BET inhibitor, we next performed a set of experiments to determine which BET is responsible for the anti-fibrotic effect of JQ1. At the mRNA level, JQ1 significantly induced *BRD2* and decreased *BRD4*, while it had minimal effect on *BRD3* (**Figure 1B**). We then knocked down BRD2, BRD3, or BRD4 individually and examined the expression of genes involved in fibrosis. As shown in **Figure 4A**, knockdown of BRD2 resulted in significant elevation of *COL1A1*, while knockdown of BRD4 led to significant reduction of *COL1A1*, *ACTA2*, *TGFB1*, *CTGF*, and *MMP1*. BRD3 knockdown decreased *TIMP3* while it had no effect on the other genes examined. We then performed gel contraction assay with the BET knocked down cells and found that only BRD4 knockdown led to significant reduction in gel contraction (**Figure 4B**), suggesting the BRD4 is pro-fibrotic, and that JQ1, by significantly reducing BRD4 expression in dcSSc fibroblasts, inhibits fibrosis in SSc.

To further confirm the involvement of BRD2 and BRD4 in myofibroblast function, we treated dcSSc fibroblasts with specific BRD2 inhibitor (B1C1) or BRD4 inhibitors (AZD5153 or ARV825). As shown in **Figure 4C**, inhibition of BRD2 by BIC1 did not

affect dcSSc fibroblast proliferation, while BRD4 inhibition by either AZD5153 or ARV825 significantly inhibited proliferation at both 1 and 10 µM. To further examine the effect of these inhibitors on fibrotic markers, we performed qPCR and Western blots after cells were treated with these inhibitors. After 48 hrs, dcSSc fibroblasts treated with BRD4 inhibitors ARV825 or AZD5153 significantly reduced *ACTA2* expression but not *COL1A1* (**Figure 4D**). In addition, BRD2 inhibitor BIC1 did not affect both *COL1A1* and *ACTA2* expression. Similar results were observed at the protein level; αSMA was significantly downregulated by BRD4 inhibitors but not by the BRD2 inhibitor (**Figure 4E**). Collagen I levels were not significantly altered in all treatments. These results further confirm the involvement of BRD4 in promoting fibrosis in dcSSc fibroblasts.

Discussion

The increased understanding of the effect of epigenetic aberrations on gene transcription has led the field to a better appreciation of the role of transcriptional dysregulation in initiating and perhaps maintaining SSc fibrosis. In this study we performed an in-depth examination of BET inhibition in SSc fibrosis. We demonstrated that JQ1 suppressed *ACTA2*, *COL1A1* and *CTGF* expression, while it increased *MMP1* in dcSSc fibroblasts and reversed the established progression of myofibroblast differentiation. Inhibition of BETs was also effective in blocking the pro-fibrotic effect of TGFβ-treated normal fibroblasts. The *in vivo* studies showed that administration of JQ1 prevented skin scarring induced by bleomycin in mice. Moreover, results from siRNA knockdown experiments confirmed the role of BRD4 in SSc fibrosis. This was further confirmed using BRD4 specific inhibitors. Together, these results suggest that BRD4 is critically involved in promoting fibrosis in SSc, and inhibition of BRD4 would be an effective treatment for this disease.

JQ1, a first in-class BET inhibitor, competitively binds to the acetyl-lysine recognition area of these proteins, and displaces them from acetylated chromatin thereby represses transcription of target genes. Early studies suggested that JQ1 exerted high anti-proliferative properties in multiple myeloma via cell-growth arrest and senescence in a c-MYC-dependent manner (14). Since then, more studies have shown the benefits of JQ1 in other proliferative disorders. In addition, this pan-BET inhibitor has demonstrated great efficacy in blocking fibrotic progression in a range of fibrosis models (5-8). In a lung fibrosis model, JQ1 significantly reduced collagen deposition in bleomycin-treated mice compared to control mice (8). This drug also ameliorated the

phenotypic changes of lung fibroblasts from idiopathic pulmonary fibrosis patients. We showed in this study that JQ1 inhibits proliferation of dcSSc dermal fibroblasts through inducing cell cycle arrest and apoptosis. It also exhibits potent anti-fibrotic effects in patient-derived cells and in the bleomycin skin fibrosis model. Our results echo the findings from Shin et al, where they showed that JQ1 repressed collagen expression in SSc skin organ culture, likely due to the increase in MMP1 (15).

BET proteins are located in the nucleus. Because of their involvement in various cellular processes, BETs have been shown to participate in tumor development, autoimmunity, infections, and inflammation (16-19). Specifically, BRD4 has been studied extensively for its role in gene transcription, including regulation (through acetylated histones), initiation (via engaging RNA polymerase II), and elongation (by interaction with P-TEFb) (20). Indeed, BRD4 is reported to control various fibrosis-related genes, including *ACTA2* (encoding αSMA) and *COL1A1*, shown from BRD4 knockdown studies or ChIP analyses (5, 7, 8, 21). This is not surprising, as both genes are reported to possess acetylated histones in their promoter region in fibroblasts (**Supplemental Figure 1**). In dcSSc fibroblasts, inhibition of BETs by JQ1 downregulated both *ACTA2* and *COL1A1*, and this appears to be mediated through blockade of BRD4, as BRD4 knockdown or inhibition led to decreased *ACTA2* and *COL1A1* levels, while knockdown of BRD2 or BRD3 did not. Interestingly, *TGFB1*, which was significantly upregulated by JQ1, was downregulated in BRD4 knocked down cells. Similar results were seen in *MMP1* expression. This discrepancy suggests that JQ1, as a pan-BET inhibitor, has off-target effects compared to BRD4 knockdown, especially at the higher concentrations. Of note, our results of BRD2 knockdown leading

to *COL1A1* elevation agrees with previous reports (21). Since JQ1 dose-dependently increased *BRD2* expression in dcSSc fibroblasts, it is possible that the anti-fibrotic effect of JQ1 is partly mediated by enhancing the anti-fibrotic potential of BRD2. However, BRD2 inhibition, although trending to induce fibroblast migration and pro-fibrotic gene expression (**Figure 4C-E**), had no significant effect on enhancing myofibroblast functions.

The molecular mechanisms of BET inhibition on tissue fibrosis have been studied extensively. These histone readers have been shown to control tissue fibrosis by regulating multiple gene programs and biochemical pathways. Inhibition of BETs suppressed various pro-fibrotic signaling networks, including the TGFβ and the EGFR/PDGFR pathway (5, 6). In addition, JQ1 blocked transactivation of genes that were robustly enriched for NF-kB and TGFβ signaling networks, including ones involved in innate immunity and myocardial fibrosis in animal models of heart failure (22). BET inhibition also appears to attenuate oxidative stress which is critical for myofibroblast differentiation (23, 24). BETs are also involved in epithelial-mesenchymal transition and endothelial-mesenchymal transition (25-27). Interestingly, BRD4 positively regulates EZH2 transcription through upregulation of c-MYC in cancer (28). In liver fibrosis, the pro-fibrotic effect of TGFβ appears to be mediated via the Smad2/BRD4/c-MYC/EZH2 pathway (29). As we previously showed that upregulated EZH2 in dcSSc fibroblasts is critical in SSc fibrosis (2), together with the above mentioned events, the anti-fibrotic effect of BET inhibition we observed in this study could arise from these mechanisms.

Due to the short half-life of JQ1, this compound is only used in preclinical studies. Currently there are several BET inhibitors with better pharmacokinetic properties in

clinical trials for various types of cancer. Recent trials also focused on targeting specific BETs, including BRD4 inhibitors AZT5153 (NCT03205176), which was used in this study, and ABBC-744 (NCT03360006). Based on our results, BETs, in particular BRD4, regulate essential processes involved in SSc fibrosis. We also highlighted the potential of epigenetic therapeutic strategies against BETs for SSc patients. These data, along with future studies focusing on the molecular mechanisms of BRD4 in SSc fibrosis, should provide the framework that supports the use of more selective BRD4 inhibitors as a therapeutic option for SSc.

Materials and Methods

Patients and Controls. All patients recruited in this study met the ACR/EULAR criteria for the classification of SSc (10). Punch biopsies from the distal forearm of healthy volunteers and diffuse cutaneous (dc)SSc patients were obtained for fibroblast isolation. This study was approved by the University of Michigan Institutional Review Board. The demographics and clinical characteristics of the enrolled individuals are summarized in **Table 1**.

Cell culture. Punch biopsies obtained from healthy subjects and SSc patients were digested as previously described (2, 11). Dermal fibroblasts were maintained in RPMI supplemented with 10% fetal bovine serum (FBS) and antibiotics. Cells between passage 3 and 6 were used in all experiments.

Cell treatment and BRD knockdown. Dermal fibroblasts from dcSSc patients were treated with 0.01-22 μM of JQ1, a pan-BET inhibitor, for 48 hours. Normal dermal fibroblasts were treated with TGFβ (10 ng/ml) and/or JQ1 (1 μM) for 72 hours to induce a myofibroblast phenotype. BRD2, BRD3, or BRD4 in dcSSc dermal fibroblasts was knocked down using *BRD2* (200nM), *BRD3* (100nM), *or BRD4* (200nM) small interfering RNA (siRNA) (ON-TARGETplus siRNA, Dharmacon) mixed with TransIT-TKO transfection reagent (Mirus Bio). Scrambled siRNA (Dharmacon) was used as a control. The cells were transfected for 72 hours before downstream experiments were performed. In a separate set of experiments, BRD2 inhibitor BIC1, BRD4 inhibitors AZD5153 or ARV825, doses ranging from 0.1-10 μM, were used to treat dcSSc fibroblasts for 48 to 72 hours.

Western blots. Cells were lysed in RIPA buffer containing protease inhibitors. Western blotting was performed following the protocol as described previously (11). After blocking the blots for an hour, the blots were probed with antibodies against BRD2, BRD3, BRD4, collagen I, and αSMA. For loading control, the blots were immunoblotted with antibodies against β-actin and GAPDH as controls. Band quantification was performed using ImageJ (12).

mRNA extraction and qRT-PCR. Total RNA was extracted using Direct-zol™ RNA MiniPrep Kit (Zymo Research). The quantity and quality of RNA were measured with a NanoDrop Spectrophotometer. The RNA was then used for synthesis of cDNA using the Verso cDNA Synthesis kit (Thermo Fisher). Quantitative PCR was performed using Power SYBR Green PCR master mix (Applied Biosystems) in a ViiA™ 7 Real-Time PCR System.

Cell proliferation assays. Proliferation of dermal fibroblasts were measured using the BrdU Cell Proliferation Assay Kit from BioVision. Cells were plated in a 96-well plate at 50,000 cell/ml and allowed to grow overnight. For dcSSc fibroblasts, cells were pre-treated with JQ1, ARV825, AZD5153, or BIC1 for 48 hours before 5-bromo-2-deoxyuridine (BrdU) was added. For normal dermal fibroblasts, cells were treated with TGFβ, JQ1, or both for 72 hours before the addition of BrdU into the wells. After 4 hours of incubation with BrdU, cells were fixed and BrdU detection antibodies were added for one hour, followed by addition of anti-mouse HRP-linked antibody after washing the wells. BrdU incorporation into cells was detected by TMB substrate and stop solution. The absorbance at 450 nm was measured using a spectrophotometer. In a separate experiment, the IncuCyte® Live-Cell Imaging System was used to monitor cell

proliferation. Cells were seeded at 5,000 cells/well and allowed to grow overnight. After adding different treatments cells were monitored by IncuCyte® up to 5 days. Cell counts were analyzed by the IncuCyte® S3 Analysis software.

Gel contraction and cell migration assays. The Cell Contraction Assay kit (Cell Biolabs) was used for gel contraction and was conducted as previously described (11). After treatment, cells were suspended at 2.5×10^6 cells/mL and mixed with collagen solution. The gel was allowed to solidify before culture media was added. Gels were lifted after 24 hours and the areas of the gels were quantified using ImageJ (12). To evaluate the effect of JQ1 on cell migration, we performed a scratch wound assay using the IncuCyte® Live-Cell Imaging System. Fibroblasts were grown to confluence and a wound gap was created using the IncuCyte® Woundmaker. After washing the cells twice with PBS, culture media with different treatments was added. Cell migration was monitored by IncuCyte® up to 7 days.

Detection of apoptosis. To assess the effect of JQ1 on cell apoptosis, cells were plated in 96 well plates and treated with JQ1 in the presence of IncuCyte® Caspase-3/7 Apoptosis Reagent (1:1000 dilution). When added to the culture medium, the non-fluorescent reagent crosses the cell membrane where it can be cleaved by activated caspase-3/7 releasing the fluorescent-stained nuclear DNA. The apoptotic cells were quantified by measuring cells with green fluorescent staining. The data were presented as green fluorescent cell number normalized with total cell count and analyzed by the IncuCyte® S3 Analysis software.

Cell cycle analysis. To evaluate the effect of JQ1 on the cell cycle of dcSSc fibroblasts, flow cytometry was performed. Fibroblasts were cultured in T75 Flasks to 75%

confluency. The fibroblasts were treated with 1 μM JQ1 for 48 hours, while the non-treated dcSSc fibroblasts were used as control. Both the JQ1 treated and non-treated cells were harvested and resuspended at 2 x 10^6 cell/mL in PBS. After fixation in 1:5 ratio of 70% ethanol, the fibroblasts were treated with 10 mg/mL RNase A (ThermoFisher) and labeled with propidium iodine (PI) in staining buffer (BioLegand). After 15 minutes of incubation at 37°C, the analysis was made with flow cytometry on ZE5 Cell Analyzer (Bio-Rad). Analysis of flow cytometry was done using FCS Express 7.

Bleomycin-induced skin fibrosis. The procedure to induce fibrosis by bleomycin in mice was published previously (2, 13). Bleomycin was dissolved to 1 mg/ml with PBS. 100 μl of bleomycin or PBS was injected subcutaneously into a single location on the shaved back of C57BL/6 mice once every day for 2 weeks. JQ1 (50 mg/kg) or vehicle control (20% DMSO/50% PBS/30% PEG) was given daily by oral gavage. At the end of the experiment, skin was excised from the injection sites, fixed in 4% paraformaldehyde and embedded in paraffin. Sections were mounted and stained with Masson's trichrome. Dermal thickness was measured by analyzing the distance between the epidermal–dermal junction and the dermal–fat junction in three fields in two or more sections from each animal. Immunofluorescence was performed on sections using anti- αSMA (Abcam) or anti-F4/80 (Invitrogen) antibodies after antigen-retrieval. Collagen content in the skin was measured using the Hydroxyproline Kit from Abcam. Skin sections from injected sites were stored in RNAlater before mRNA was extracted, followed by qPCR analysis. All animal protocols were approved by the Institutional Animal Care & Use Committee at the University of Michigan.

Statistical analysis. To determine the differences between groups, Mann–Whitney U test, Wilcoxon test, Kruskal–Wallis test, or two-way ANOVA were performed using GraphPad Prism version 8 (GraphPad Software, Inc). P values of less than 0.05 were considered statistically significant. Results were expressed as mean ± SD.

Funding info: This work was supported by the funds from the American Autoimmune Related Disease Foundation and the Edward T. and Ellen K. Dryer Early Career Professorship (Tsou), National Institute of Arthritis and Musculoskeletal and Skin Diseases grant K24 AR063120 (Khanna) and R01 AR070148 (Sawalha).

References

1. P. S. Tsou, Epigenetic Control of Scleroderma: Current Knowledge and Future Perspectives. *Curr Rheumatol Rep* **21**, 69 (2019).
2. P. S. Tsou *et al.*, Inhibition of EZH2 prevents fibrosis and restores normal angiogenesis in scleroderma. *Proc Natl Acad Sci U S A* **116**, 3695-3702 (2019).
3. C. Bergmann *et al.*, The histone demethylase Jumonji domain-containing protein 3 (JMJD3) regulates fibroblast activation in systemic sclerosis. *Ann Rheum Dis* **77**, 150-158 (2018).
4. M. Kramer *et al.*, Inhibition of H3K27 histone trimethylation activates fibroblasts and induces fibrosis. *Ann Rheum Dis* **72**, 614-620 (2013).
5. C. Xiong *et al.*, Pharmacological targeting of BET proteins inhibits renal fibroblast activation and alleviates renal fibrosis. *Oncotarget* **7**, 69291-69308 (2016).
6. B. Zhou *et al.*, Brd4 inhibition attenuates unilateral ureteral obstruction-induced fibrosis by blocking TGF-beta-mediated Nox4 expression. *Redox Biol* **11**, 390-402 (2017).
7. N. Ding *et al.*, BRD4 is a novel therapeutic target for liver fibrosis. *Proc Natl Acad Sci U S A* **112**, 15713-15718 (2015).

8. X. Tang *et al.*, BET bromodomain proteins mediate downstream signaling events following growth factor stimulation in human lung fibroblasts and are involved in bleomycin-induced pulmonary fibrosis. *Molecular pharmacology* **83**, 283-293 (2013).

9. A. Alqahtani *et al.*, Bromodomain and extra-terminal motif inhibitors: a review of preclinical and clinical advances in cancer therapy. *Future Sci OA* **5**, FSO372-FSO372 (2019).

10. F. van den Hoogen *et al.*, 2013 classification criteria for systemic sclerosis: an American college of rheumatology/European league against rheumatism collaborative initiative. *Ann Rheum Dis* **72**, 1747-1755 (2013).

11. P. S. Tsou, D. Khanna, A. H. Sawalha, Identification of Cysteine-Rich Angiogenic Inducer 61 as a Potential Antifibrotic and Proangiogenic Mediator in Scleroderma. *Arthritis Rheumatol* **71**, 1350-1359 (2019).

12. C. A. Schneider, W. S. Rasband, K. W. Eliceiri, NIH Image to ImageJ: 25 years of image analysis. *Nat Methods* **9**, 671 (2012).

13. D. J. Kahl *et al.*, 5-Aryl-1,3,4-oxadiazol-2-ylthioalkanoic Acids: A Highly Potent New Class of Inhibitors of Rho/Myocardin-Related Transcription Factor (MRTF)/Serum Response Factor (SRF)-Mediated Gene Transcription as Potential Antifibrotic Agents for Scleroderma. *J Med Chem* **62**, 4350-4369 (2019).

14. J. E. Delmore *et al.*, BET bromodomain inhibition as a therapeutic strategy to target c-Myc. *Cell* **146**, 904-917 (2011).

15. J. Y. Shin *et al.*, Epigenetic activation and memory at a TGFB2 enhancer in systemic sclerosis. *Science Translational Medicine* **11**, eaaw0790 (2019).

16. K. Klein, Bromodomain protein inhibition: a novel therapeutic strategy in rheumatic diseases. *RMD Open* **4**, e000744 (2018).

17. J. L. Morgado-Pascual, S. Rayego-Mateos, L. Tejedor, B. Suarez-Alvarez, M. Ruiz-Ortega, Bromodomain and Extraterminal Proteins as Novel Epigenetic Targets for Renal Diseases. *Frontiers in pharmacology* **10**, 1315 (2019).

18. F. Mietton *et al.*, Selective BET bromodomain inhibition as an antifungal therapeutic strategy. *Nature Communications* **8**, 15482 (2017).

19. G. P. Andrieu *et al.*, BET proteins in abnormal metabolism, inflammation, and the breast cancer microenvironment. *Journal of leukocyte biology* **104**, 265-274 (2018).

20. B. Donati, E. Lorenzini, A. Ciarrocchi, BRD4 and Cancer: going beyond transcriptional regulation. *Molecular Cancer* **17**, 164 (2018).

21. K. Kumar *et al.*, BET inhibitors block pancreatic stellate cell collagen I production and attenuate fibrosis in vivo. *JCI Insight* **2**, e88032 (2017).

22. Q. Duan *et al.*, BET bromodomain inhibition suppresses innate inflammatory and profibrotic transcriptional networks in heart failure. *Sci Transl Med* **9** (2017).

23. C. J. W. Stock *et al.*, Bromodomain and Extraterminal (BET) Protein Inhibition Restores Redox Balance and Inhibits Myofibroblast Activation. *Biomed Res Int* **2019**, 1484736 (2019).

24. M. Qu *et al.*, BRD4 inhibitor JQ1 inhibits and reverses mechanical injury-induced corneal scarring. *Cell Death Discovery* **4**, 64 (2018).

25. X. Wang *et al.*, Bromodomain-containing protein 4 contributes to renal fibrosis through the induction of epithelial-mesenchymal transition. *Exp Cell Res* **383**, 111507 (2019).

26. S. Song *et al.*, Inhibition of BRD4 attenuates transverse aortic constriction- and TGF-beta-induced endothelial-mesenchymal transition and cardiac fibrosis. *J Mol Cell Cardiol* **127**, 83-96 (2019).

27. B. Tian *et al.*, BRD4 mediates NF-kappaB-dependent epithelial-mesenchymal transition and pulmonary fibrosis via transcriptional elongation. *Am J Physiol Lung Cell Mol Physiol* **311**, L1183-L1201 (2016).

28. X. Wu *et al.*, BRD4 Regulates EZH2 Transcription through Upregulation of C-MYC and Represents a Novel Therapeutic Target in Bladder Cancer. *Mol Cancer Ther* **15**, 1029-1042 (2016).

29. X. Cai *et al.*, CXCL6-EGFR-induced Kupffer cells secrete TGF-beta1 promoting hepatic stellate cell activation via the SMAD2/BRD4/C-MYC/EZH2 pathway in liver fibrosis. *J Cell Mol Med* **22**, 5050-5061 (2018).

Figure legends

Figure 1. Inhibition of BETs by JQ1 affects genes involved in fibrosis. (A) BET proteins bind to acetylated histones to promote gene transcription. We hypothesize that BET proteins promote pro-fibrotic gene expression in SSc and that inhibition of BETs by JQ1 inhibits fibrosis. **(B)** At doses between 0.01-22 µM, JQ1 significantly down-regulated *ACTA2*, *COL1A1*, *CTGF* and *BRD4* in dcSSc fibroblasts, while it significantly upregulated *MMP1*, *TGFB1*, and *BRD2*. It did not affect *TIMP1* and *BRD3*. n=number of patients. Results are expressed as mean +/- SD and $p<0.05$ was considered significant.

Figure 2. Inhibition of BETs shows potent anti-fibrotic properties. (A) Migration of dcSSc fibroblasts was significantly inhibited by JQ1. Cell migration was monitored by IncuCyte® Live-cell imaging. Wound confluence indicates the number of cells migrated into the wound gap. **(B)** Inhibition of BETs by JQ1 significantly reduced cell proliferation of dcSSc fibroblasts. Cell growth was analyzed by BrdU uptake in cells or monitored by IncuCyte® Live-cell imaging. **(C)** JQ1 induced significant cell apoptosis in dcSSc fibroblasts. Apoptosis was measured by a green fluorescence dye that couples with activated caspase 3/7 in cells. Apoptotic cell count and total cell numbers were monitored by IncuCyte® Live-cell imaging. Data was presented as number of apoptotic cells normalized by total cell count. Representative result from 3 patient lines. **(D)** JQ1 (1µM) induced cell cycle arrest in dcSSc fibroblasts; it induced cell accumulation in G1 phase and a decrease in S phase. **(E)** Gel contraction by dcSSc fibroblasts was

inhibited by JQ1 at 0.5 µM. **(F-H)** Cell migration, proliferation, and gel contraction significantly increased after TGFβ treatment in normal dermal fibroblasts, and can be inhibited by co-incubation of 1 µM of JQ1. **(I)** Bleomycin-treated mice showed increased dermal thickness and hydroxyproline content in skin, and JQ1 (50mg/kg) efficiently prevented skin fibrosis in these mice. **(J)** Immunofluorescent staining of skin sections showed trends of increase in αSMA-positive cells (green) in bleomycin-treated mice compared to the PBS group, and decrease in JQ1-treated mice. Similar results were found quantifying F4/80-positive cells (red). Significant increase in F4/80-positive cells was observed in bleomycin-treated mice, and these cells were decreased with JQ1 treatment. Nuclei were stained with DAPI (blue). n=number of patients or animals. Results are expressed as mean +/- SD and $p<0.05$ was considered significant.

Figure 3. The expression of BET proteins is not altered in dcSSc compared to normal fibroblasts. (A) At the mRNA levels, *BRD2* and *BRD3* were similar in normal and dcSSc fibroblasts, while *BRD4* was significantly upregulated in dcSSc fibroblasts. **(B)** At the protein level, BRD2, BRD3, and BRD4 showed variable levels in dcSSc, however there was no difference between normal and dcSSc fibroblasts when the bands were quantified. n=number of patients. Results are expressed as mean +/- SD and $p<0.05$ was considered significant.

Figure 4. BRD4 mediates the pro-fibrotic effect of BETs. (A) BRD2 knockdown in dcSSc fibroblasts led to upregulation of *COL1A1* while BRD3 knockdown resulted in downregulation of *TIMP3*. Knockdown of BRD4 resulted in downregulation of *COL1A1*,

ACTA2, *TGFB*, *CTGF*, and *MMP1*. **(B)** BRD4 knockdown significantly inhibited gel contraction in dcSSc fibroblasts while BRD2 or BRD3 knockdown had minimal effect on gel contraction. **(C)** Treating dcSSc fibroblasts with specific BRD2 inhibitor BIC1 had minimal effect on cell proliferation, while inhibition of BRD4 using BRD4 inhibitors AZD5153 or ARV825 significantly reduced cell proliferation at concentrations of 1 and 10 µM. **(D)** Inhibition of BRD4 by ARV825 or AZD5153 in dcSSc fibroblasts significantly reduced *ACTA2* expression but not *COL1A1*. Inhibition of BRD2 by BIC1 had no effect on *COL1A1* and *ACTA2* expression. **(E)** BRD4 inhibitors significantly decreased αSMA in dcSSc fibroblasts while BRD2 inhibition by BIC1 had minimal effect. n=number of patients. Results are expressed as mean +/- SD and $p<0.05$ was considered significant.

Table 1: SSc patients and healthy controls characteristics.

	dcSSc (n=33)	Healthy volunteers (n=21)
Age (years)	54.5 ± 2.9[a]	56.4 ± 3.3
Sex	F24/M9	F11/M10
Disease duration (years)	3.2 ± 0.6	N.A.
Modified Rodnan Skin Score	20.3 ± 2.2	N.A.
Raynaud's phenomenon	33	N.A.
Early disease (< 5yrs)	29	N.A.
Interstitial lung disease	18	N.A.
Pulmonary arterial hypertension	9	N.A.
Immunosuppressive	30	N.A.

[a]Mean ± SEM
[b]N.A. = Not applicable

Table 2: The mRNA expression levels of selected target genes in mice treated with bleomycin and/or JQ1. Data shown as mean +/- S.D and p-value<0.05 denotes significance. *p<0.05 vs. PBS; ¥p<0.05 vs. bleomycin.

Gene	PBS (n=8-9)	Bleomycin (n=12)	Bleomycin+JQ1 (n=9)
Col1a1	0.680 ± 0.561	2.649 ± 2.229*	0.727 ± 0.939¥
Acta2	0.026 ± 0.035	0.148 ± 0.142*	0.038 ± 0.059¥
Ctgf	0.051 ± 0.047	0.089 ± 0.084	0.066 ± 0.098

A

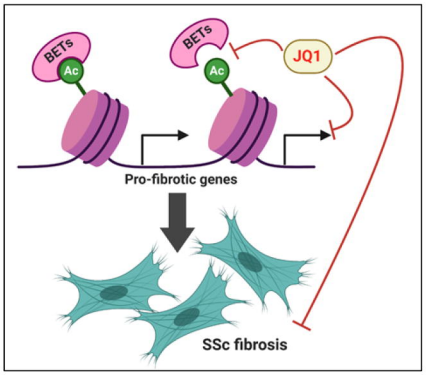
BETs
Ac
BETs
Ac
JQ1
Pro-fibrotic genes
SSc fibrosis

B

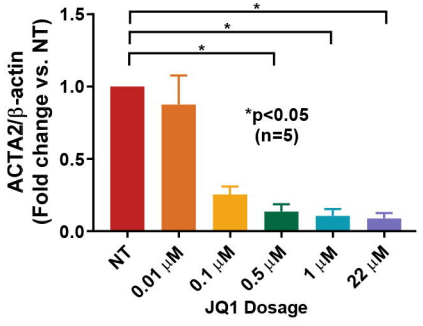
ACTA2/β-actin
(Fold change vs. NT)
*p<0.05
(n=5)
NT
0.01 μM
0.1 μM
0.5 μM
1 μM
22 μM
JQ1 Dosage

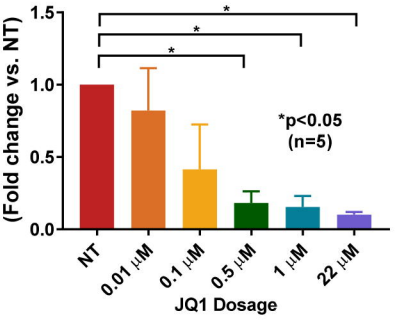
COL1A1/β-actin
(Fold change vs. NT)
*p<0.05
(n=5)
NT
0.01 μM
0.1 μM
0.5 μM
1 μM
22 μM
JQ1 Dosage

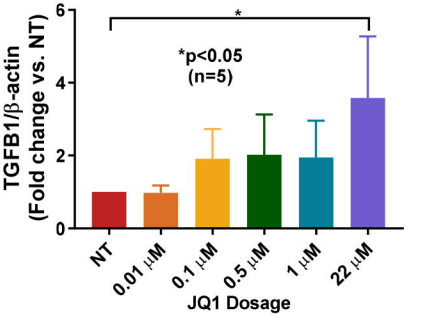
TGFB1/β-actin
(Fold change vs. NT)
*p<0.05
(n=5)
NT
0.01 μM
0.1 μM
0.5 μM
1 μM
22 μM
JQ1 Dosage

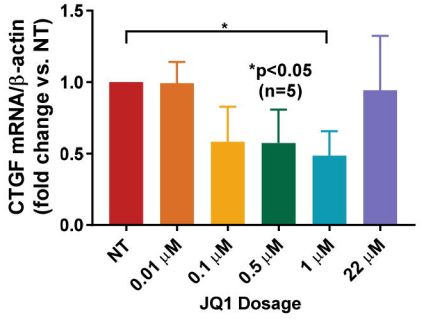
CTGF mRNA/β-actin
(fold change vs. NT)
*p<0.05
(n=5)
NT
0.01 μM
0.1 μM
0.5 μM
1 μM
22 μM
JQ1 Dosage

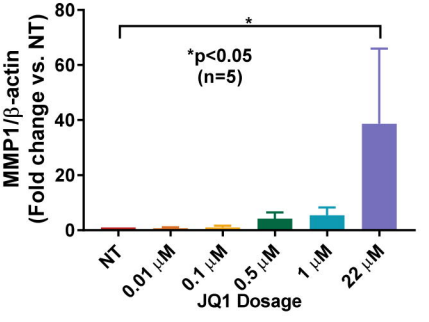
MMP1/β-actin
(Fold change vs. NT)
*p<0.05
(n=5)
NT
0.01 μM
0.1 μM
0.5 μM
1 μM
22 μM
JQ1 Dosage

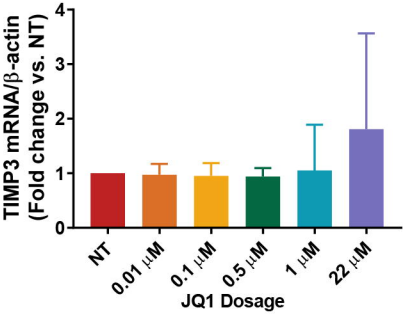
TIMP3 mRNA/β-actin
(Fold change vs. NT)
NT
0.01 μM
0.1 μM
0.5 μM
1 μM
22 μM
JQ1 Dosage

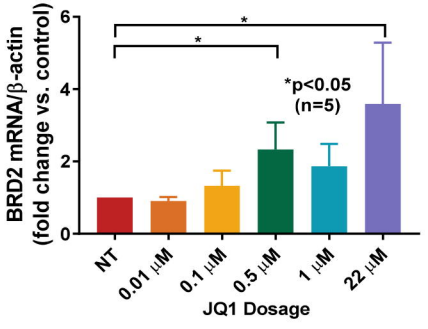
BRD2 mRNA/β-actin
(fold change vs. control)
*p<0.05
(n=5)
NT
0.01 μM
0.1 μM
0.5 μM
1 μM
22 μM
JQ1 Dosage

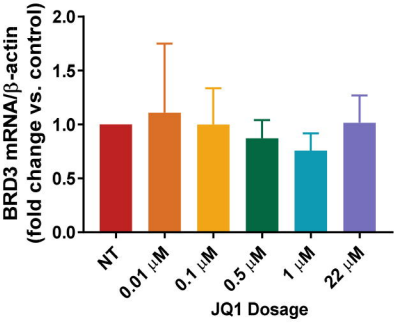
BRD3 mRNA/β-actin
(fold change vs. control)
NT
0.01 μM
0.1 μM
0.5 μM
1 μM
22 μM
JQ1 Dosage

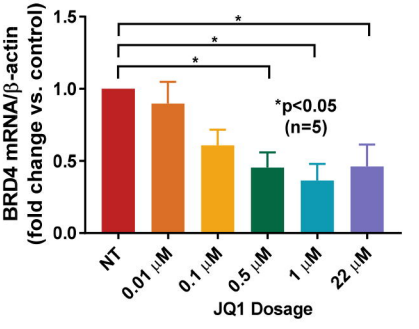
BRD4 mRNA/β-actin
(fold change vs. control)
*p<0.05
(n=5)
NT
0.01 μM
0.1 μM
0.5 μM
1 μM
22 μM
JQ1 Dosage

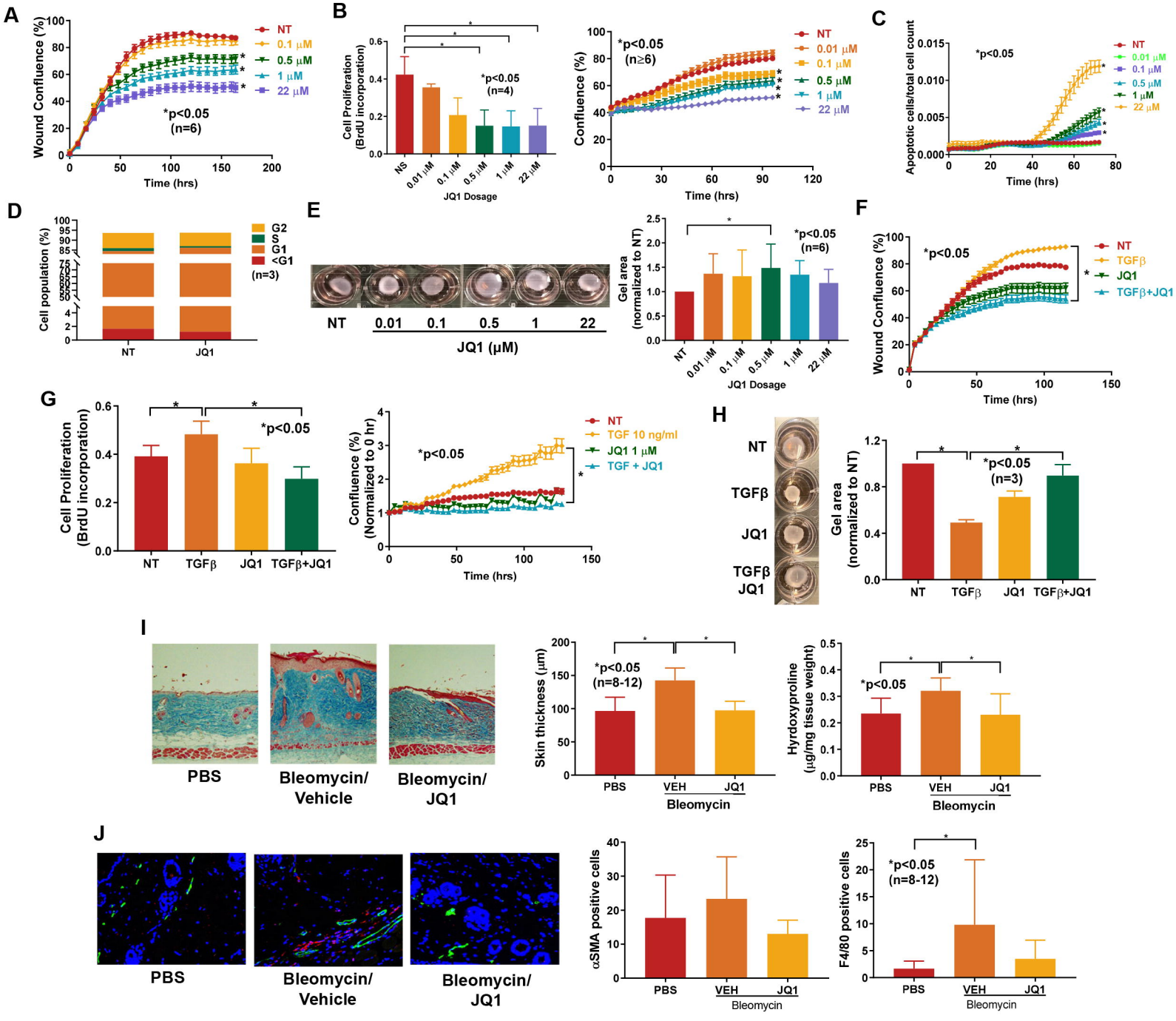
A
Wound Confluence (%)
Time (hrs)
NT
0.1 μM
0.5 μM
1 μM
22 μM
*p<0.05
(n=6)
B
Cell Proliferation
(BrdU incorporation)
JQ1 Dosage
NS
0.01 μM
0.1 μM
0.5 μM
1 μM
22 μM
*p<0.05
(n=4)
Confluence (%)
Time (hrs)
*p<0.05
(n≥6)
C
Apoptotic cells/total cell count
Time (hrs)
*p<0.05
D
Cell population (%)
G2
S
G1
<G1
(n=3)
NT
JQ1
E
NT
0.01
0.1
0.5
1
22
JQ1 (μM)
Gel area
(normalized to NT)
JQ1 Dosage
*p<0.05
(n=6)
F
Wound Confluence (%)
Time (hrs)
*p<0.05
NT
TGFβ
JQ1
TGFβ+JQ1
G
Cell Proliferation
(BrdU incorporation)
NT
TGFβ
JQ1
TGFβ+JQ1
*p<0.05
Confluence (%)
(Normalized to 0 hr)
Time (hrs)
*p<0.05
NT
TGF 10 ng/ml
JQ1 1 μM
TGF + JQ1
H
NT
TGFβ
JQ1
TGFβ
JQ1
Gel area
(normalized to NT)
*p<0.05
(n=3)
NT
TGFβ
JQ1
TGFβ+JQ1
I
PBS
Bleomycin/
Vehicle
Bleomycin/
JQ1
Skin thickness (μm)
*p<0.05
(n=8-12)
PBS
VEH
JQ1
Bleomycin
Hyrdoxyproline
(μg/mg tissue weight)
*p<0.05
PBS
VEH
JQ1
Bleomycin
J
PBS
Bleomycin/
Vehicle
Bleomycin/
JQ1
αSMA positive cells
PBS
VEH
JQ1
Bleomycin
F4/80 positive cells
*p<0.05
(n=8-12)
PBS
VEH
JQ1
Bleomycin

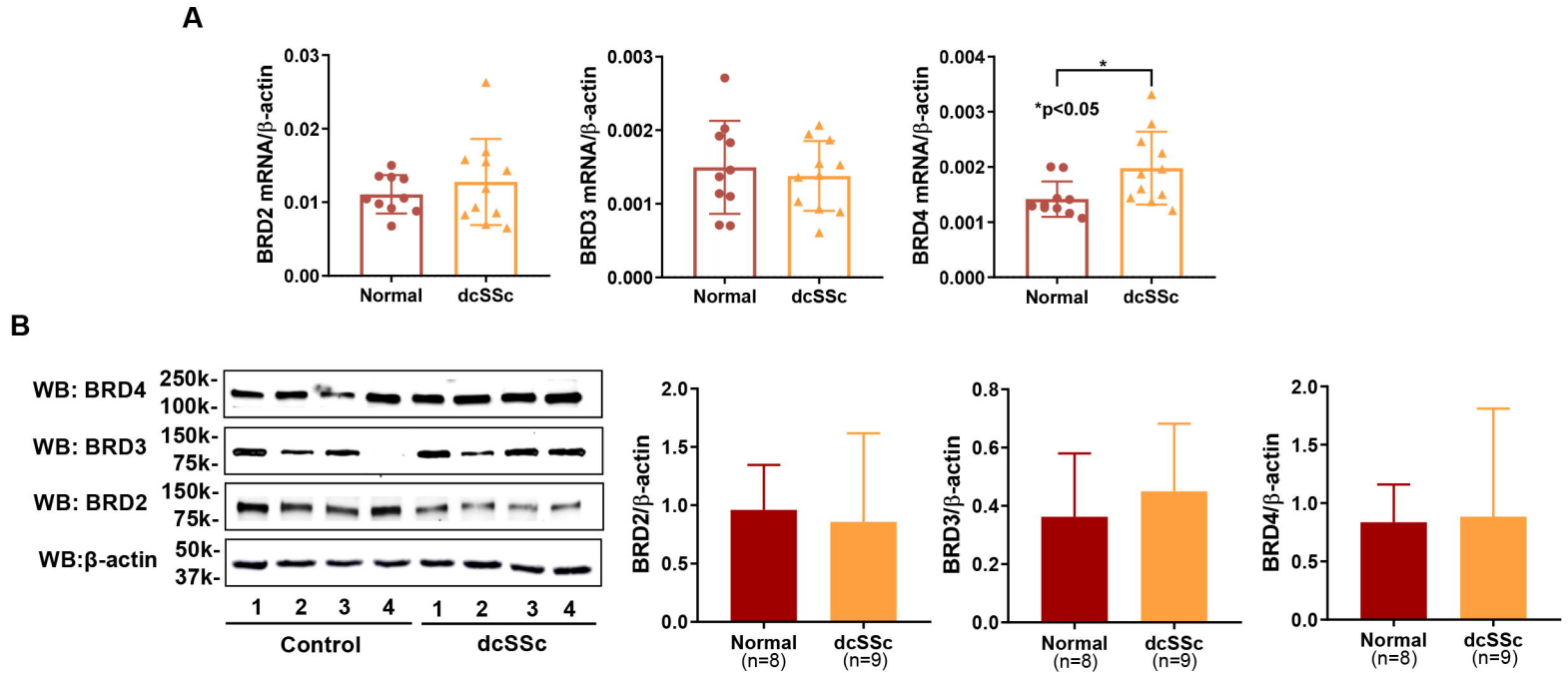
A
BRD2 mRNA/β-actin
0.03
0.02
0.01
0.00
Normal
dcSSc
BRD3 mRNA/β-actin
0.003
0.002
0.001
0.000
Normal
dcSSc
BRD4 mRNA/β-actin
0.004
0.003
0.002
0.001
0.000
*
*p<0.05
Normal
dcSSc
B
WB: BRD4
250k-
100k-
WB: BRD3
150k-
75k-
WB: BRD2
150k-
75k-
WB:β-actin
50k-
37k-
1 2 3 4 1 2 3 4
Control
dcSSc
BRD2/β-actin
2.0
1.5
1.0
0.5
0.0
Normal (n=8)
dcSSc (n=9)
BRD3/β-actin
0.8
0.6
0.4
0.2
0.0
Normal (n=8)
dcSSc (n=9)
BRD4/β-actin
2.0
1.5
1.0
0.5
0.0
Normal (n=8)
dcSSc (n=9)

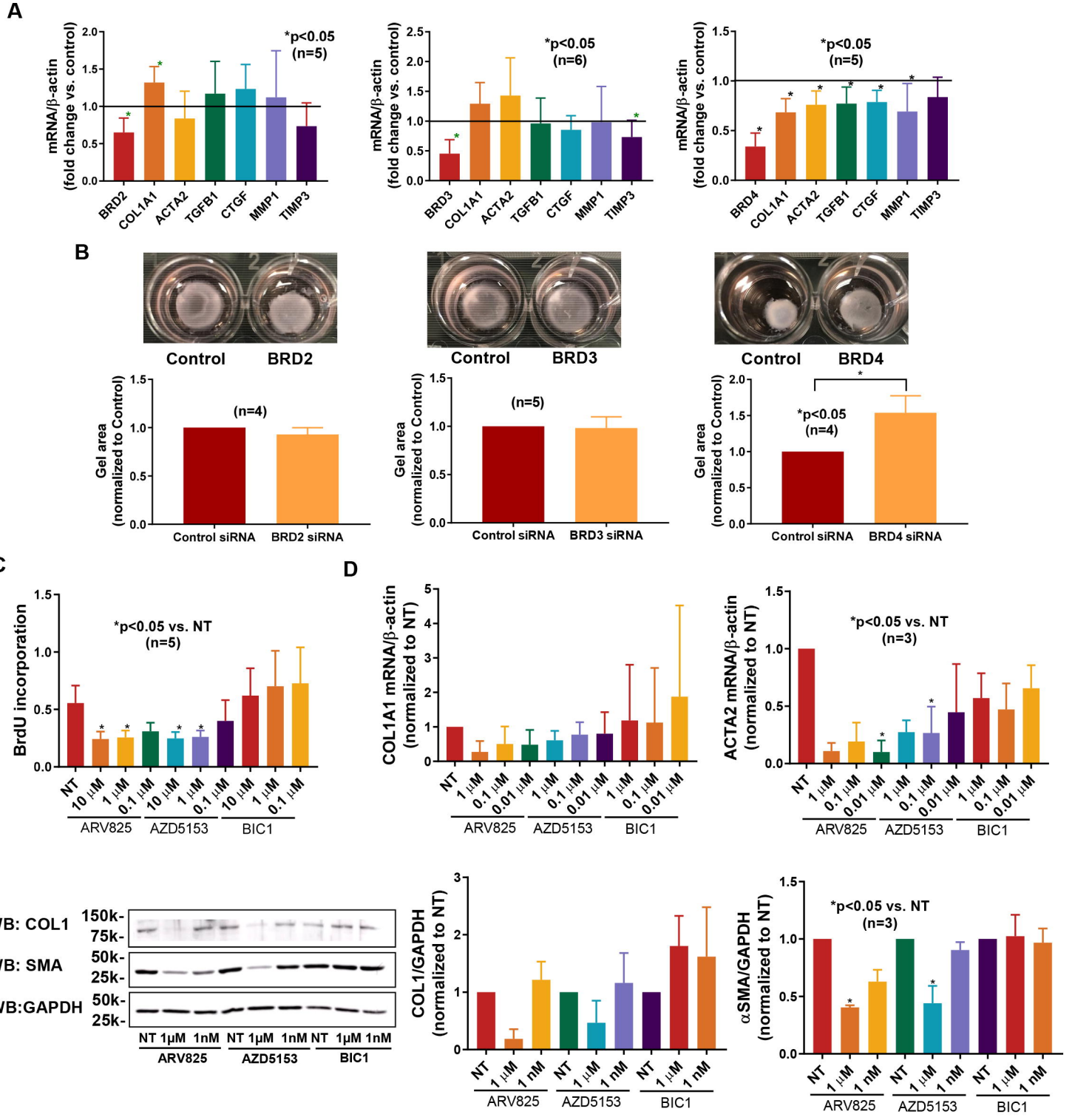
A
mRNA/β-actin (fold change vs. control)
*p<0.05 (n=5)
BRD2 COL1A1 ACTA2 TGFB1 CTGF MMP1 TIMP3
*p<0.05 (n=6)
BRD3 COL1A1 ACTA2 TGFB1 CTGF MMP1 TIMP3
*p<0.05 (n=5)
BRD4 COL1A1 ACTA2 TGFB1 CTGF MMP1 TIMP3
B
Control BRD2
Control BRD3
Control BRD4
Gel area (normalized to Control)
(n=4)
Control siRNA BRD2 siRNA
(n=5)
Control siRNA BRD3 siRNA
*p<0.05 (n=4)
Control siRNA BRD4 siRNA
C
BrdU incorporation
*p<0.05 vs. NT (n=5)
NT 10 μM 1 μM 0.1 μM
ARV825 AZD5153 BIC1
D
COL1A1 mRNA/β-actin (normalized to NT)
NT 1 μM 0.1 μM 0.01 μM
ARV825 AZD5153 BIC1
ACTA2 mRNA/β-actin (normalized to NT)
*p<0.05 vs. NT (n=3)
E
WB: COL1
WB: SMA
WB:GAPDH
150k-
75k-
50k-
25k-
NT 1μM 1nM
ARV825 AZD5153 BIC1
COL1/GAPDH (normalized to NT)
αSMA/GAPDH (normalized to NT)
*p<0.05 vs. NT (n=3)